



## EXPERIMENTAL STUDY AND RELIABILITY ASSESSMENT OF A SELF-CENTERING STEEL BEAM DURING ITS DESIGN SERVICE LIFE

Pu Yang<sup>(1)</sup>, Yiming Yang<sup>(2)</sup>, Minghao Hu<sup>(3)</sup>, Peiwen Shen<sup>(4)</sup>, Zongming Huang<sup>(5)</sup>

<sup>(1)</sup> Professor, School of Civil Engineering, Chongqing University, P. R. China, yangpu1009@163.com

<sup>(2)</sup> PhD student, School of Civil Engineering, Chongqing University, P. R. China, yangym@cqu.edu.cn

<sup>(3)</sup> Master student, School of Civil Engineering, Chongqing University, P. R. China, hmh19930908@126.com

<sup>(4)</sup> PhD student, School of Civil Engineering, Chongqing University, P. R. China, peiwen Shen@163.com

<sup>(5)</sup> Professor, School of Civil Engineering, Chongqing University, P. R. China, zmhuang@cqu.edu.cn

### Abstract

To eliminate structural damage and residual deformation after earthquake events, a new type of steel Self-Centering Beam (SCB) is developed in this paper which capacity of restoring force and energy dissipation is provided by Post-Tensioned (PT) strands and Buckling Restrained Steel (BRS) plates, respectively. A steel Self-Centering Moment Resisting Frame (SCMRF) of 1-story 1-bay and pinned connections at column bases is designed, and its beam is SCB using different BRS plates. Then the experiments of SCMRF under cyclic loading were conducted to investigate their seismic behavior. The experimental results demonstrated that properly designed frames were able to undergo lateral displacement up to 4% story drift while the columns and beam remained elastic. Also, the BRS plates showed good energy dissipation capacity by yielding in tension and compression without fracture. Structural damage was limited to the replaceable BRS plates. Then an analytical model was constructed in OpenSees and its effectiveness was verified by experimental results. The reliability of SCB section corresponding to ultimate limit state was evaluated using JC method and its reliability index was also calculated which illustrate that the designed SCB satisfy the requirement of current Chinese code, Unified standard for reliability design of building structures. Finally, development tendency of reliability for the SCB during its whole service life was predicted considering structural resistance change due to corrosion and relaxation of PT strands, and material deterioration of BRS plates etc. the results shown that reliability index of SCB will decreased significantly in first 1 service year, while its annual dropping ratio decreases year by year, and the probability of failure for SCB will increased from 0.26% to 0.51% after 50 years later.

*Keywords: Self-Centering, Residual deformation, Energy dissipation, Reliability assessment, Design service life*



## 1. Introduction

According to conventional seismic design strategy, balance of strength and ductility for a structure is required, thus seismic energy is mainly dissipated by structural members and severe damage may occur after earthquake event. Consequently, it's difficult and costly repair and recover its function of the structure after earthquake. Therefore, seismic design approach of self-centering (SC) system is proposed recently to reduce or eliminate residual deformation and protect structural components from seismic damage. In SC structural system, the seismic energy would be dissipated by replaceable energy dissipate devices instead of structural component, and the system might return to its original position because of unbonded Post-tensioned (PT) strands.

The design methodology of Self-Centering moment-resisting steel frame was initially proposed and developed by Garlock & Ricles et al [1]. Post-tensioning strands are used to clamp the beams to column. During an earthquake, the post-tensioned connections decompress and develop a gap-opening which leads to effective softening of lateral force-drift behavior without or with minor damage to structural members. The restoring force is provided by PT strands and energy is dissipated by supplemental elements named ED Fuse, such as yielding angles or friction dampers [2-3].

A new Self-Centering Beam (SCB) is proposed and developed [4-6]. Its configuration and deformation shape subjected to lateral loading are shown in Fig. 1. It consists of W-section beam, inner tube, outer tube, post-tensioning (PT) strands, free floating anchorage plates and Buckling Restrained Steel (BRS) plates. The outer tube is not connected to the moment frame columns and welded to the bottom flange of W-section beam, so the beam will cause the outer tube to push right anchorage plate to move right, while the inner tube is connected to the columns and moves laterally relative to the outer tube. Thus distance between two anchorage plates increases and results in gap opening, PT strands pre-compress the concentric tubes and encourage the inner and outer tubes to be aligned. Then the telescopic movement between the two tubes cause the BRS plates to deform axially and dissipate energy.

So its capacity of restoring force and energy dissipation is provided by PT strands and BRS plates, respectively. Then, a steel Self-Centering Moment Resisting Frame (SCMRF) of 1-story 1-bay and pinned connections at column bases is designed, and its beam is SCB using different BRS plates. Then the experiments of SCMRF under cyclic loading were conducted to investigate their seismic behavior.

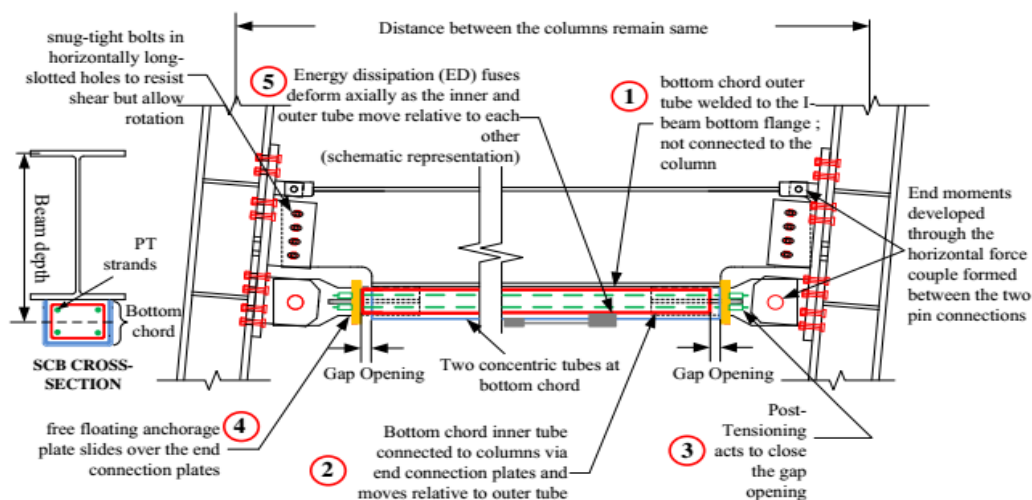


Fig. 1 Description of SCB subjected to lateral loading

Many research works focus on seismic performance, design method of SC system and parameters influence of ED fuse and PT strands etc. rather than reliability assessment although it is also important for



structure safety. Therefore, in this paper, an analytical model is constructed using OpenSees and its effectiveness was verified by comparison of analysis and experimental results, then the reliability of SCB section corresponding to ultimate limit state was evaluated using JC method. Finally, development tendency of reliability for the SCB during its whole service life was predicted considering structural resistance change due to corrosion and relaxation of PT strands, and material deterioration of BRS plates etc.

## 2. Theoretical behavior of SCB

The expected behavior of PT strand, BRS plates and SCB subjected to cyclic loading is shown in Fig. 2. There are a few key events under lateral loading: 1) Elastic stage, its lateral stiffness is similar as conventional moment frame since there is no gap-opening occurred at this stage. 2) Gap development stage, the gap-opening of anchorage plate is observed and BRS plate does not yield. 3) ED fuse yielding stage, BRS plates yield and dissipates energy through their deformation and the gap of anchorage plate develops. 4) Self-centering stage, the frame returns to its original position with negligible residual drift.

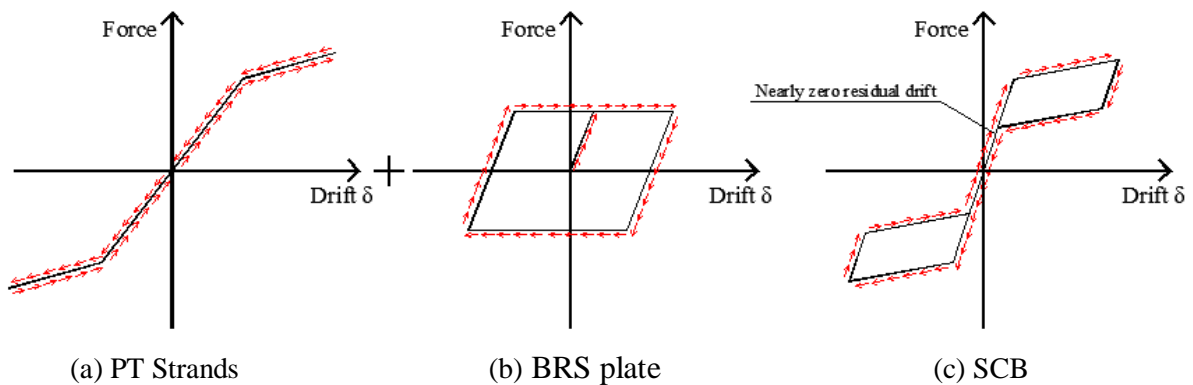


Fig. 2 Behaviour of SCB

Taken the SCB as two free body diagrams, shown as Fig. 3, the first part is the W-section beam and outer tube and the second part is the inner tube.

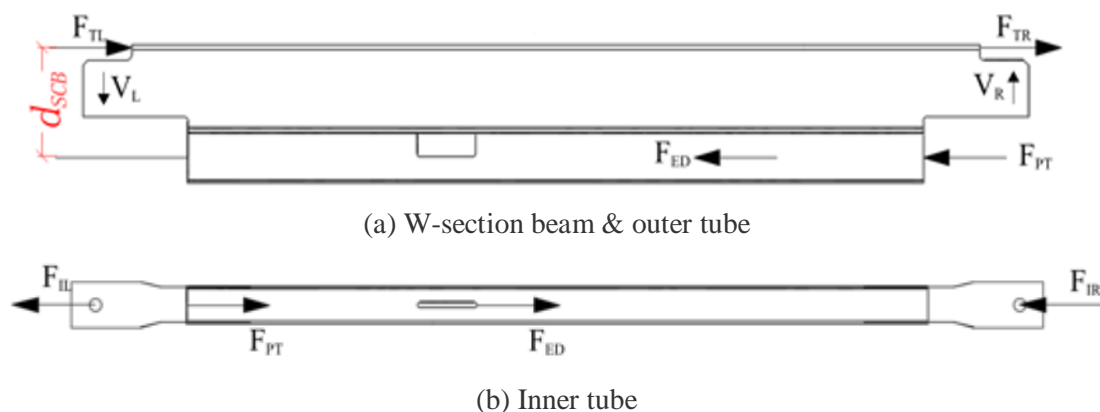


Fig. 3 Free body diagrams

When the SCB frame is subjected to lateral cyclic loading, W-section beam and inner tube suffered horizontal force ( $F_{TR}$  and  $F_{TL}$  on beam,  $F_{IL}$  and  $F_{IR}$  on outer tube), equilibrium equation is as follows:

$$F_{TL} + F_{TR} = F_{IL} + F_{IR} \quad (1)$$



After the gap-opening has occurred, the anchorage plate bears on the outer tube on the right end and inner tube on the left hand. Thus, the force due to PT strands ( $F_{PT}$ ) as well as  $F_{ed}$  is exerted on the inner tube at the right end and outer tube at the left end of the SCB. For first part, equilibrium equation is as Eq. (2):

$$F_{TL} + F_{TR} = F_{PT} + F_{ED} \quad (2)$$

The moments caused by the horizontal force couples at each end of the SCB, shown as  $M_L$  and  $M_R$ . Note that the fuses and the PT strands work along the same line of force (centroid of the concentric tubes) and hence the moment lever arm for both the forces is  $d_{SCB}$ .

$$M = M_L + M_R = \frac{(F_{TR} + F_{IR} + F_{TL} + F_{IL})d_{SCB}}{2} = (F_{ED} + F_{PT})d_{SCB} \quad (3)$$

During the test, assuming rigid body motion of the whole frame, the strain in the PT strand is calculated based on the story drift of the moment frame since the PT strand did not yield.

$$\varepsilon_{PT} = \frac{F_{PT,in}}{A_{PT}E_{PT}} + \frac{(\theta - \theta_{open})d_{SCB}}{L_{eff}} \quad (4)$$

Where,  $\theta_{open}$  is storey drift when gap-opening occurs.  $\theta$  is storey drift.  $L_{eff}$  represents effective length of PT strands.  $F_{PT,in}$  is initial post-tension force in PT strand.  $A_{PT}$  is total cross-section area of PT strands.  $d_{SCB}$  is depth measured from the center of W-beam top flange to the centroid of the inner tube.  $E_{PT}$  represents modulus of elasticity for PT strands.

According to material test of ED fuse, its yielding strain,  $\varepsilon_{ED}$  is about 0.2%, thus the moment capacity at each end of SCB,  $M$  can be determined by following equation:

$$M = (m\sigma_{PT}A_{PT} + nf_{ED}A_{ED})d_{SCB}$$

$$= \begin{cases} \left[ m \left( \frac{F_{PT,in}}{A_{PT}E_{PT}} + \frac{(\theta - \theta_{open})d_{SCB}}{L_{eff}} \right) E_{PT}A_{PT} + n\varepsilon_{ED}E_{ED}A_{ED} \right] d_{SCB} & , \varepsilon_{ED} < 0.2\% \\ \left[ m \left( \frac{F_{PT,in}}{A_{PT}E_{PT}} + \frac{(\theta - \theta_{open})d_{SCB}}{L_{eff}} \right) E_{PT}A_{PT} + nf_{ED}A_{ED} \right] d_{SCB} & , \varepsilon_{ED} \geq 0.2\% \end{cases} \quad (5)$$

Where,  $m, n$  represents the number of PT strands and ED fuses, respectively.  $f_{y,ED}$  is nominal yield strength of ED fuse material.  $A_{ED}$  is total cross-sectional area of ED fuses

### 3. Comparison of Experiment and Simulation results of SCB Frame

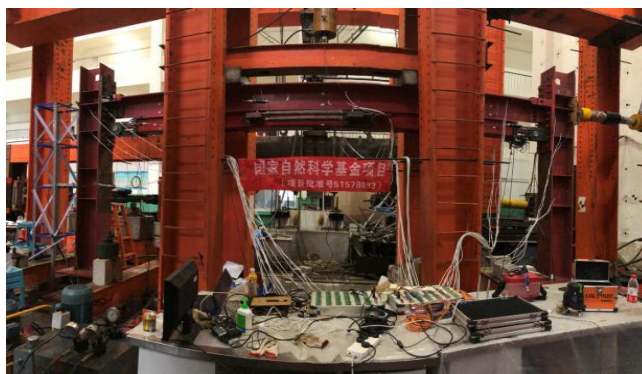
To investigate behavior of SCB, several scale-testing programs were conducted in Thomas M. Murray Structures Laboratory at Virginia Tech and Chongqing University[4-5]. The specimen are summarized in table 1.



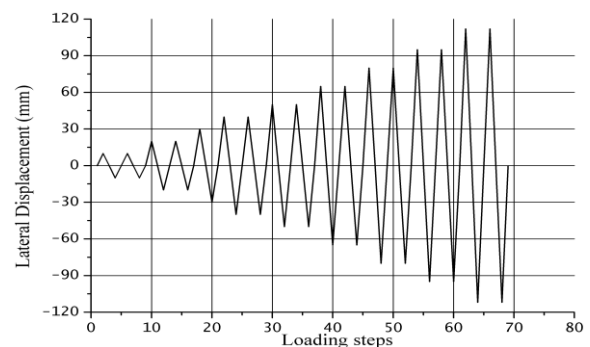
Table 1 Test matrix of SCB

Specimen	$L_{eff}$ /mm	$d_{SCB}$ /mm	$F_{PT,in}$ /kN	$A_{PT}$ /mm <sup>2</sup>	$E_{PT}$ /MPa	$A_{ED}$ /mm <sup>2</sup>	$f_{ED}$ /MPa
SCB-2F	4700	431.5	180.78	182.32	200000	227.42	280.35
SCB-3F	4700	622.3	97.67	182.32	200000	227.42	280.35
SCB-4F	4700	622.3	128.49	120.7	200000	179.03	280.35
SCB-5F	4700	622.3	86.22	182.32	200000	157.26	280.35
SCBM1.7	4600	435.5	102	137	195000	150	415
SCBM1.25	4600	435.5	94	137	195000	200	415
SCBM1.00	4600	435.5	94	137	195000	250	415
SCB-1	4600	435.5	100	137	195000	150	310
SCB-2	4600	435.5	100	137	195000	200	380
SCB-3	4600	435.5	100	137	195000	150	310
SCB-4	4600	435.5	100	137	195000	200	380

The test setup is shown in Fig. 4a. The total span of frame between columns' centerlines is 6100mm and the height of frame,  $h$  from the pinned base to position of actuator is 2800mm. The base of the columns is connected to the foundation blocks with a true pin connection. Lateral load was applied at the top of the column by a 200t actuator and vertical load used a 50t actuator. The loading protocol was controlled by top displacement as shown in Fig. 5b.



(a) Test setup



(b) Loading protocol

Fig. 4 Test setup and loading protocol

Besides experiments, a two-dimensional analytical models for specimen SCB-1, SCB-2, SCB-3 and SCB-4 was established using OpenSees shown in Fig. 5. Plastic beam-column element by fibre sections is used to simulate behaviour of columns, W-section beam and concentric tubes of SCB frame, while Truss Element with initial stress and Two-Node-Link Element is used to represent performance of PT strands and ED Fuses, respectively.

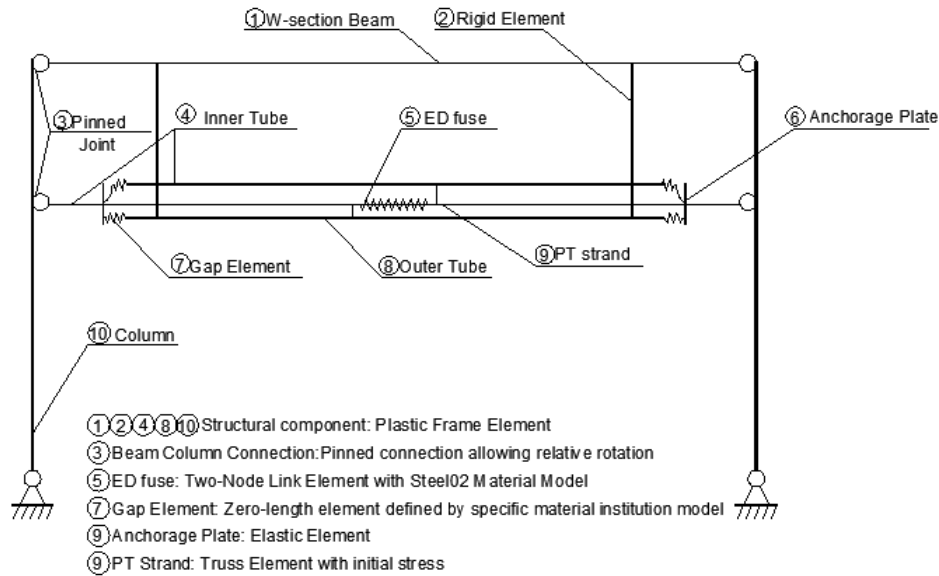


Fig. 5 Analytical model of SCB

The global behaviour of tests and simulation results (Chongqing University, 2018) were compared in Fig. 6. The lateral residual displacement was not observed and main structural components did not yield except ED fuses after cyclical loading. Meanwhile, the effectiveness and accuracy of proposed analytical model was verified by comparison of experiments and simulation results.

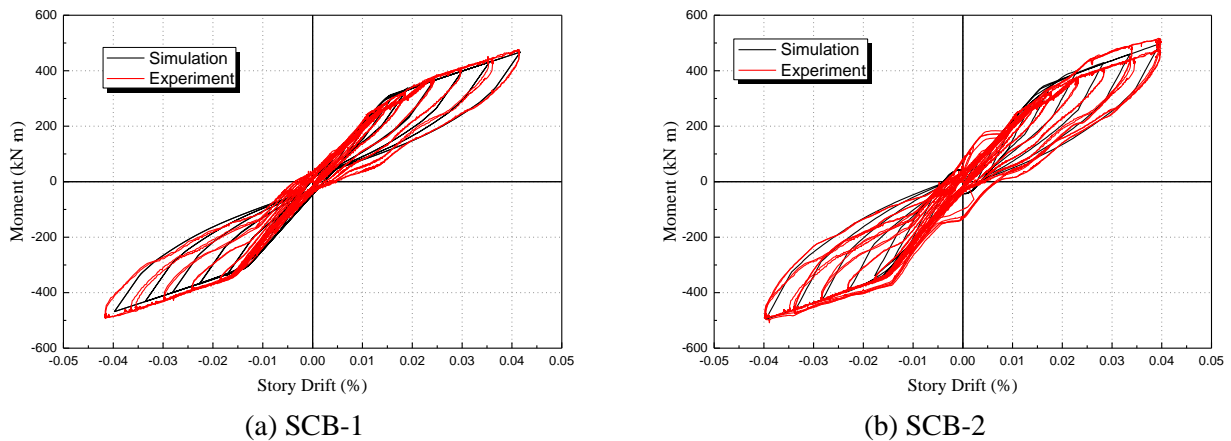


Fig.6 Comparison of global behaviour between tests and simulation results

#### 4. Reliability analysis

Reliability is a measure of probability of structural failure and can be determined using probability density functions  $g(x)$  by following equation.

$$Z = g(R, S) = R - S \quad (6)$$



Where,  $R$  and  $S$  represents variables of resistance and load effect respectively. If  $Z < 0$ , it means system failed, otherwise, it is safety. Assuming  $S$  and  $R$  follows the law of normal distribution, the probability of failure can be expressed as follows:

$$P_f = P(Z < 0) = \int_{-\infty}^0 \frac{1}{\sqrt{2\pi}\sigma_Z} \exp\left[-0.5 \times \left(\frac{z - \mu_Z}{\sigma_Z}\right)^2\right] dz = \Phi\left(\frac{-\mu_Z}{\sigma_Z}\right) = \Phi(-\beta) \quad (7)$$

In addition, reliability index  $\beta$  can be expressed as Eq. 8,

$$\beta = \frac{\mu_Z}{\sigma_Z} = \frac{\mu_R - \mu_S}{\sqrt{\sigma_R^2 + \sigma_S^2}} \quad (8)$$

Where,  $\mu_R$  and  $\mu_S$  are mean values of  $R$  and  $S$ , while  $\sigma_R$  and  $\sigma_S$  are standard deviation of  $R$  and  $S$  respectively. Based on probability theory, relation between  $P_f$  and  $\beta$  can be expressed as follows:

$$P_r = 1 - P_f = 1 - \Phi(-\beta) = \Phi(\beta) \quad (9)$$

For a traditional seismic designed structure, its limit states under earthquake excitation can be provided by current codes, but for reliability analysis of a SCB, it is necessary to define limit states. since it is hard to observe damage among structures components except yielding of ED fuses. Meanwhile, SCB has good ductility and self-centering ability even if its lateral drift is over 4%. Therefore, the limit state of SCB was defined as yielding of ED fuse because the lateral displacement of SCB meets requirement of current seismic design code when ED fuse yields[8,9].

#### 4.1 Resistance models

There are three factors affecting the distribution of Resistance: martial factor  $M$ , fabrication factor  $F$  and uncertainty factor about calculation model  $P$ . Generally, these variables are assumed to follow lognormal distribution, Then the resistance  $R$  can be expressed as Eq. (10)

$$R = R_n \times M \times F \times P \quad (10)$$

Where,  $R_n$  is nominal resistance capacity;  $M$  refers to uncertainty of material properties due to structural processing technology, load condition, surrounding environment and other factors.  $F$  expresses variability in geometrical parameters of components caused by dimensional deviations and mounting errors compare with their designed size.  $P$  is ratio of actual resistance value to theoretical one.

Statistical parameters of  $M$  and  $F$  were gotten from previous research works as shown in Table 2 and Table 3, respectively.

Table 2. Parameters of factors  $M$  in moment equation

Variables	Standard value, $R_n$	Mean factor, $\mu_M$	Coefficient of variation, $\delta_M$
$F_{PT,in}$	100 kN	1.03	0.03
$E_{PT}$	195000 MPa	1.03	0.01
$f_{y,ED}$	235 MPa	1.30	0.09

Table 3. Parameters of factor  $F$  in moment equation

Variables	Standard value, $R_n$	Mean factor, $\mu_F$	Coefficient of variation, $\delta_F$
$L_{eff}$	4600 mm	1.00	0.00
$d_{SCB}$	435.5 mm	1.00	0.00
$A_{PT}$	137 mm <sup>2</sup>	1.00	0.024
$A_{ED}$	150 mm <sup>2</sup>	1.01	0.01
$\theta_{open}$	1.44% rad	1.00	0.00
$\theta_{y,ED}^*$	1.56% rad	1.00	0.00

Note: \* drift when yielding of ED fuse occurs.

While statistical parameter of  $P$  was taken from experimental and predicted value corresponding to ultimate limit state shown in Table 4.

Table 4. Parameters of factor  $P$  in SCB

Specimen	Experimental moment, $Ma$	Predicted moment, $Mp$	$P=Ma/Mp$	Mean factor, $\mu_P$	Coefficient of variation, $\delta_P$
SCB-2F[6]	459.88 kp.ft	410.61 kp.ft	1.12	1.16	0.0029
SCB-3F[6]	566.15 kp.ft	501.02 kp.ft	1.13		
SCB-4F[6]	489.22 kp.ft	414.59 kp.ft	1.18		
SCB-1FF[7]	453.58 kp.ft	394.42 kp.ft	1.15		
SCBM1.7[7]	360.75 kN.m	325.00 kN.m	1.11		
SCBM1.25[7]	376.99 kN.m	316.80 kN.m	1.19		
SCBM1.00[7]	404.26 kN.m	348.50 kN.m	1.16		
SCB-1	303.25 kN.m	257.52 kN.m	1.18		
SCB-2	352.72 kN.m	298.41 kN.m	1.18		
SCB-3	362.30 kN.m	295.32 kN.m	1.23		
SCB-4	406.32 kN.m	356.87 kN.m	1.14		

Based on above statistics data, the mean and variation coefficient of resistance capacity could be calculated as following equations:

$$\mu_R = R_n \times \mu_M \times \mu_F \times \mu_P \quad (10a)$$

$$\delta_R = \sqrt{\delta_M^2 + \delta_F^2 + \delta_P^2} \quad (10b)$$



## 4.2 Factors related to reliability during SCB service life

There are a few factors affecting probability of SCB during its service life, such as corrosion of PT strands, stress relaxation of PT strands and resistance degradation of ED fuse etc.

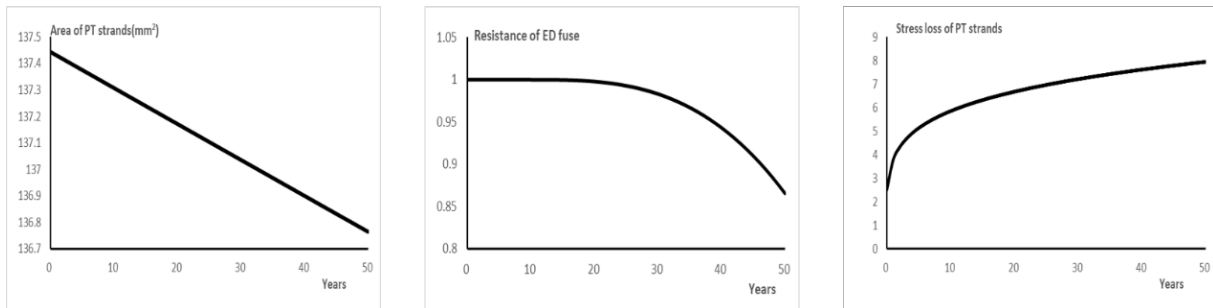
Corrosion of PT strands refers to deterioration of its section area caused by environmental medium (such as water, air, etc.). Generally, it is assumed uniform, for example, LI [10] proposed a predicted equation to calculate available sectional area of PT strands as follows.

$$A_{st}(t) = \begin{cases} 7\pi r^2, & 0 \leq t \leq t_s \\ 4\pi r^2 + 3\pi[r - \Delta r(t)]^2, & t_s \leq t \leq r / 0.0116i_{corr} \end{cases} \quad (11)$$

Where  $r$  is initial radius of PT strands, and radius decreases  $\Delta r$  can be expressed as:

$$\Delta r(t) = 0.0116i_{corr}(t - t_s) \quad (12)$$

Where,  $t_s$  is start time of corrosion, taken  $t_s=0$  in this case;  $t$  is current time, unit: second;  $i_{corr}$  is a coefficient related to environment, taken 0.025. The curve of PT strand area under corrosion during design period (50 years) is shown in Fig. 7a.



(a) Corrosion of PT strands      (b) Relaxation of PT strands      (c) Degradation of ED fuse

Fig. 7 Changing curves of considered factors

Stress relaxation of PT strands refers to its stress decrease after long time under constant environment conditions (i.e. temperature and loading, etc). CBE-FIP proposed a predicted equation to estimate the stress loss in PT strands. [11-13]

$$p_t = \left( p_{1000} \frac{t}{1000} \right)^K \quad (13)$$

Where,  $p_t$  is the relaxing rate after  $t$  hours,  $t$  is duration time of relaxation,  $p_{1000}$  is the relaxing rate after 1000 hours;  $p_{1000}=2.5\%$ ;  $K$  is time coefficient, taken as 0.19. Stress loss of PT strands during design period is shown in Fig. 7b.

If ED fuse is made of steel, its real-time function related to steel fuse resistance is interfered by surrounding environment such as corrosion and loading types. Yang [14] proposed a degradation function for steel structure given in Eq. 14.



$$\varphi(t)_{steel} = \left\{ 1 - \left[ 0.7 \times \frac{(t - t_c)^3}{10000} \right] \times 0.04 \times \alpha \times \varepsilon \right\} \times (1 - t^2 \times r^2) \quad (14)$$

Where,  $t_c$  is effective time of anti-corrosion measures, considering the protection of outer tube of ED fuse.  $\alpha$  represents steel coefficient;  $\varepsilon$  refers environment coefficient;  $r$  is loading coefficient. in the paper,  $t_c$  is 10 years,  $\alpha=1$  for normal steel,  $\varepsilon=0.75$ ,  $r=0$  for static loading, thus degradation equation of ED fuse is given as Eq. (15) and the changing curve is shown in Fig 7c.

$$\varphi(t)_{steel} = 1 - \left[ 0.7 \times \frac{(t - 10)^3}{10000} \right] \times 0.04 \quad (15)$$

### 4.3 Beam section moment equation in its design period

Considering Corrosion, Stress relaxation of PT strands and resistance degradation of ED fuse, moment capacity equation of SCB section during the design period is given as follows:

$$M = (M_{PT} + M_{ED})\varphi(t)$$

$$= \begin{cases} \left[ m \left( \frac{F_{PT,in}}{A_{st}(t)E_{PT}} + \frac{(\theta - \theta_{open})d_{SCB}}{L_{eff}} \right) E_{PT}A_{st}(t)(1 - p_t) + n\varepsilon_{ED}E_{ED}bw\varphi(t)_{steel} \right] d_{SCB}, & \varepsilon_{ED} \leq 0.15\% \\ \left[ m \left( \frac{F_{PT,in}}{A_{st}(t)E_{PT}} + \frac{(\theta - \theta_{open})d_{SCB}}{L_{eff}} \right) E_{PT}A_{st}(t)(1 - p_t) + nf_{ED}bw\varphi(t)_{steel} \right] d_{SCB}, & \varepsilon_{ED} > 0.15\% \end{cases} \quad (16)$$

### 4.4 Load effect models

As discussed, load effect  $S$  only considers moment caused by seismic action. Gao proposed a mathematic method to convert seismic actions to base shear force based on the distribution of seismic action and structural dynamic characteristics. Since the connection between the column foot and base is pinned, the distribution of base shear force is the same as beam end moment. The distribution of load followed extreme value I distribution. The biased factor is 1.06 and coefficient of variation is 0.3.

### 4.5. Reliability index and Probability of failure of SCB

FOSM method, First Order and Second Moment method, is widely used to evaluate Probability of structure failure and calculate reliability index in engineering field. However, traditional FOSM method has its limitations, leading to large error particularly when variables do not follow normal distributions, so JC method is proposed based on FORM, its basic idea is to normalize the non-normally distributed random variables to become normal distribution variables and it is able to get an approximate calculation of the reliability index  $\beta$  with high accuracy. In this paper, JC method is used to calculate the changing reliability of SCB. Table 5 shows the results.



Table 5 Reliability parameters in SCB

Designed period/year	0	1	10	20	30	40	50
Reliability index	2.8	2.74	2.71	2.65	2.63	2.60	2.57
Probability of failure %	0.26	0.31	0.34	0.40	0.43	0.47	0.51

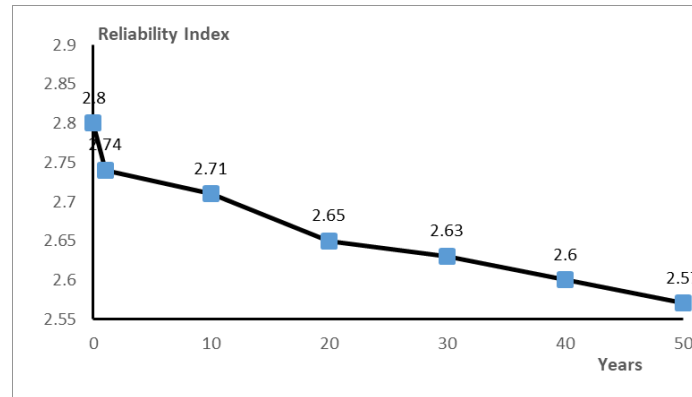


Fig. 8 Changing curve of reliability of SCB

## 5. Conclusions

The experimental results demonstrated that properly designed frames were able to undergo lateral displacement up to 4% story drift while the columns and beam remained elastic. And structural damage was limited to the replaceable BRS plates.

The reliability of SCB section corresponding to ultimate limit state was evaluated using JC method and its reliability index was also calculated which illustrate that the designed SCB satisfy the requirement of current Chinese code, Unified standard for reliability design of building structures.

Development tendency of reliability for the SCB during its whole service life was predicted considering structural resistance change due to corrosion and relaxation of PT strands, and material deterioration of BRS plates etc. the results shown that reliability index of SCB will decreased significantly in first 1 service year, while its annual dropping ratio decreases year by year, and the probability of failure for SCB will increased from 0.26% to 0.51% after 50 years later.

## 6. Acknowledgements

This paper is based on research works supported by the National Natural Science Foundation of China, Project No. 51578093 and Chongqing Natural Science Foundation, Project No. cstc2018jcyjA2863. I also appreciate Mr. Jiawei Yang for reviewing English writing of the paper.

## 7. Copyrights

17WCEE-IAEE 2020 reserves the copyright for the published proceedings. Authors will have the right to use content of the published paper in part or in full for their own work. Authors who use previously published data and illustrations must acknowledge the source in the figure captions.



## 8. References

References must be cited in the text in square brackets [1, 2], numbered according to the order in which they appear in the text, and listed at the end of the manuscript in a section called References, in the following format:

- [1] Ricles J M, Sause R, Garlock M M, et al (2001). Post-tensioned seismic-resistant connections for steel frames. *Journal of Structural Engineering*, 127(2), 113-121.
- [2] Garlock M M, Ricles J M, Sause R (2005). Experimental studies of full-scale posttensioned steel connections. *Journal of Structural Engineering*, 131(3), 438-448.
- [3] Garlock M M, Sause R, Ricles J M (2007). Behavior and design of posttensioned steel frame systems. *Journal of Structural Engineering*, 133(3), 389-399.
- [4] Chancellor, B., Eatherton, M.R., Roke, D., Akbaş, T. (2014). Self-Centering Seismic Lateral Force Resisting Systems: High Performance Structures for the City of Tomorrow. *Buildings*, Vol. 4, No. 3, pp. 520-548.
- [5] Yang Pu, Gao haojie, et al. Analysis of stress mechanism and seismic behavior of a new self-centering steel truss beam. *Journal of Civil, Architectural & Environmental Engineering*, 2018, 40(02): 12-18 (In Chinese).
- [6] Christopoulos, C., Tremblay, R., Kim, H.J. And Lacerte, M. (2008), Self-centering energy dissipative bracing system for the seismic resistance of structures: development and validation, *Journal of Structural Engineering*, ASCE, 134: 96-107.
- [7] Abhilasha Maurya (2014). Experimental and Computational Investigation of a Self-centering Beam Moment Frame (SCB-MF) [D]. Virginia Polytechnic Institute and State University
- [8] Zhao Guofan, Jin Weiliang, Gong Jinxin (2000). Structural reliability theory. *China Building Industry Press*. (In Chinese).
- [9] Gao Xiaowang, Bao aibin (1985). Probability model of earthquake action and its statistical parameters. *Earthquake Engineering and Engineering Vibration*, 1985(01): 13-22 (In Chinese).
- [10] Li Tian, Gao Minghui, et al (2005). Investigation and Analysis of the Uncertainty of Main Geometrical Dimensions of Steel Components. *Journal of Zhengzhou University (Science Edition)*, (01): 87-90 (In Chinese).
- [11] Chen Zhihua, Liu zhanxing (2010). Study on the partial coefficient of cable resistance and reliability analysis. *Journal of Building Structure*, 31(S1): 241-246 (In Chinese).
- [12] Darmawan M S, Stewart M G (2007). Spatial time-dependent reliability analysis of corroding pretensioned prestressed concrete bridge girders. *Structural Safety*, 2007(29): 16-31
- [13] Mao Aiju (2013). Relaxation test of prestressed steel strand and calculation of long-term relaxation value. *Academic Committee of Metal Products of China Metal Society Rolling Steel Branch*. 2013:8 (In Chinese).
- [14] Yang Bo, Dai Guoxin, et al (2008). Construction and verification of time-varying model of steel structure engineering resistance. *Journal of Chongqing Jianzhu University*, 2008(05):95-99 (In Chinese).